Journal of Sound and Vibration 328 (2009) 428–440

Contents lists available at ScienceDirect

Journal of Sound and Vibration

journal homepage: www.elsevier.com/locate/jsvi

Free vibration analysis of delaminated beams using mixed finite element model

G.S. Ramtekkar *

Department of Civil Engineering, National Institute of Technology Raipur, Raipur (C.G.)-492 010, India

ARTICLE INFO

Article history:
Received 10 May 2007
Received in revised form
29 March 2009
Accepted 11 August 2009
Handling Editor: J. Lam
Available online 27 August 2009

ABSTRACT

Free vibration analysis of laminated beams with delamination has been presented in this paper. A 2-D plane stress mixed finite element model developed by the authors [G.S. Ramtekkar, Y.M. Desai, A.H. Shah, Natural vibrations of laminated composite beams by using mixed finite element modeling, *Journal of Sound and Vibration* 257(4) (2002) 635–641.] has been employed. Two models, namely the *unconstrained-interface model* and the *contact-interface model* have been proposed for the computation of frequencies and the mode shapes of delaminated beams. Laminated beams with mid-plane delamination as well as off-mid-plane delamination have been considered and the results have been compared with various theoretical and experimental results available in the literature. It has been concluded that the *contact-interface model* presents a realistic behaviour of the dynamics of delaminated beams whereas the *unconstrained-interface model* under-predicts the frequencies, particularly at the higher modes

1. Introduction

Advanced composite materials are finding increasing application in aircraft, automobiles, marine and submarine vehicles besides other engineering applications owing to their high specific strength and stiffness. Consequently, these applications have stimulated interest in the development of mathematical models for prediction of the dynamic behaviour of the physical models with sufficient accuracy. Moreover, all these applications of composite materials in advanced technology areas, where precision and reliability play a paramount role, demand clear understanding of their behaviour and performance under severe operating environments.

One of the commonly encountered types of defects or damage in laminated composite structures is delamination. Delaminations may originate during fabrication or may be service-induced, such as by impact of fatigue loading. Delaminations not only affect the strength and integrity of the structure but also cause the reduction of the stiffness, thus affecting its vibration and stability characteristics. This paper presents a study on the effect of delamination on the vibration characteristics of laminated beams.

Wang et al. [2] performed the free vibration analysis of the isotropic beams with split at the mid-plane by developing an analytical model. The model allows the free deformation of upper and lower layer at the split location. Mujumdar and Suryanarayan [3] presented two models namely the *free mode model* and the *constrained mode model* for the flexural vibrations of isotropic beams with delamination at the mid-plane as well as at the off-mid-plane locations. Experimental results have also been presented for various cases of delaminations in the beams. The paper concluded that the *constrained*

* Tel.: +91 771 2255423; fax: +91 771 2254600.
E-mail address: rsgdr@indiatimes.com

0022-460X/$ - see front matter © 2009 Elsevier Ltd. All rights reserved.
doi:10.1016/j.jsv.2009.08.008

Nomenclature

a, h	length and depth (thickness) of a laminate
$[D]$	constitutive matrix with reference to the element reference axes x, y, z
D_{ij}	coefficients of constitutive matrix with reference to the element reference axes x, z
E_1, E_3	Young's moduli of lamina in the material principal directions 1, 3
G_{13}	Shear moduli of a lamina
$[K]^e$, $[K]$	element property matrix and global property matrix, respectively
$[L]$	derivative matrix
L^e, T^e, U^e	total energy, kinetic energy and strain energy of an element
$2L_x$, $2L_z$	element's dimensions
$[M]^e$, $[M]$	element inertia matrix and global inertia matrix, respectively
$[N]$	shape function matrix
$\{q\}$, $\{Q\}$	element degree-of-freedom vector and global degree-of-freedom vector, respectively
s	aspect ratio of the laminate $= a/h$
T	time
$[T_d]$	transformation matrix
u, w	displacement components along element's reference axes x, z
$\underline{u}$ or $\{u\}$	displacement vector
$\bar{U}$, $\bar{W}$	non-dimensionalized displacement components along laminate's reference axes X, Z
U, W	displacement components along laminate's reference axes X, Z
x, z	Cartesian coordinate system for an element (local coordinates)
X, Z	Cartesian coordinate system for a laminate (global coordinates)
$\bar{X}$, $\bar{Z}$	X/a, Z/h (non-dimensionalized dimensions of laminate)
1, 3	Cartesian coordinate system for a lamina; the fibre direction and the transverse to fibre directions (material principal directions)
α	inclination of the fibres of a lamina with the positive direction of laminate X-axis, measured in anticlockwise direction
$\underline{\varepsilon}$ or $\{\varepsilon\}$	strain vector
ε_x, ε_z, γ_{xz}	components of strain with respect to the element's reference axes x, z
ε_1, ε_3, γ_{13}	components of strain with respect to the lamina's reference axes 1, 3
ε_X, ε_Z, γ_{XZ}	components of strain with respect to the laminate's reference axes X, Z
ν_{ij}	Poisson's ratio
ξ, η	X/L_x and z/L_z, respectively
ρ	mass density
$\underline{\sigma}$ or $\{\sigma\}$	stress vector
σ_x, σ_z, τ_{xz}	components of stress with respect to the element's reference axes x, z
σ_1, σ_3, τ_{13}	components of stress with respect to the lamina's reference axes 1, 3
σ_X, σ_Z, τ_{XZ}	components of stress with respect to the laminate's reference axes X, Z
$\bar{\sigma}_Z$, $\bar{\tau}_{XZ}$	non-dimensionalized/normalized components of the stress at a point within a laminate with respect to the laminate's reference axes X, Z
ω	natural frequency
$\bar{\omega}$	non-dimensionalized natural frequency

mode model in which the transverse displacement and the normal stress of the upper and lower layer at the delaminated interface have been constrained to be the same, gives results in good consonance with the experimental results. The *free mode model* (similar to the one developed by Wang [2]) under-predicts the frequencies, particularly at the higher modes.

Tracy and Pardoen [4] presented the experimental modal analyses of simply supported beams to find out the effect of delamination on the natural frequencies of composite laminates. Further, the experimental results are corroborated by detailed finite element model based on the classical beam theory. Shen and Grady [5] presented experimental and analytical results for the free vibrations of multilayer laminated beam with delamination of various lengths, located at different interfaces. The paper presents two analytical models. In the first model the crack interfaces have been assumed to be in contact along the delaminated region throughout the vibration and the coupling effect has been accounted for in both the upper and lower plies in the delaminated region. In the second model, the contact between the delamination surfaces has been neglected. It has been shown that the frequencies obtained through the first model are in better agreement with the experimental results. An analytical model based on the Timoshenko beam theory has been presented by Hu and Hwu [6] for the free vibrations of delaminated sandwich beams. The natural frequencies and the mode shapes of the delaminated composite sandwich beams have been presented in the paper.

Krawczuk et al. [7] presented finite element model for the analysis of natural frequencies of delaminated composite beams. The influence of the length of delamination and its position on the bending natural frequencies of laminated cantilever beam has been investigated in the paper. Lee [8] presented a displacement-based layer-wise finite element model for the analysis of free vibration of delaminated beam. Numerical results showing the effects of the lamination angle, location, size and number of delamination have been presented. A review paper on the vibration-based model-dependent damage (delamination) identification and health monitoring for composite structures has been presented by Zou et al. [9]. The paper deals with various models proposed for the free vibrations of delaminated beams. Karmakar et al. [10] presented the effect of delamination on free vibration characteristics of graphite-epoxy composite pre-twisted shallow shells of various stacking sequences considering length of delamination as a parameter. An exhaustive review on the vibration of delaminated composites has been presented Della et al. [11]. The paper deals with various analytical models

and numerical analysis for the free vibration of composite laminates. Della et al. [12] developed analytical solutions to study the free vibrations of multiple delaminated beams under axial compressive loadings. The Euler–Bernoulli beam theory and free mode and constrained mode assumption in delamination buckling and vibration are used in the analysis.

Various FE models presented in the literature for the free vibrations of delaminated beams are based on the conventional displacement-based finite element models. Moreover, they are based on either the classical beam theory or the first order shear deformation theories (i.e. Timoshenko beam theory). It has already been pointed out by the authors [1] that the mixed layer-wise FE models represent the behaviour of laminated structures more appropriately because of the better modeling of the kinetics and kinematics of laminated structures. The present analysis has been performed using the plane-stress mixed FE model described in [1], which has been developed using the Hamilton's principle. The model ensures the through thickness continuity of the transverse stress and the displacement components. In addition, it also ensures the fundamental elastic relations between the stress and the displacement fields throughout the elastic continuum. This is particularly an important feature of the model, which is lacking in various mixed FE model developed using various *multi-field* variational principles. Because the FE model has transverse stresses as the nodal degrees-of-freedom in addition to the displacement variables, appropriate boundary conditions at the delaminated interface can be enforced.

2. Theoretical formulation

2.1. Formulation of mixed finite element model

A detailed formulation has been presented in [1], however for sake of completeness and also for ready reference the formulation has been breafly described here.

An anisotropic composite laminated beam consisting of N-layers of orthotropic lamina has been considered for FE analysis shown in Fig. 1(a,b). The beam has been discretized into a number of plane stress elements. Each element lies completely within a lamina and no element crosses the interface between any two successive laminae.

A six-node plane stress mixed finite element model shown in Fig. 1(c) has been developed by considering the displacement fields $u(x,z,t)$ and $w(x,z,t)$ having quadratic variation along longitudinal axis x and cubic variation along transverse axis z. The displacement fields can be expressed as

$$u_k(x,z) = \sum_{i=1}^{3} g_i a_{0ik} + z\sum_{i=1}^{3} g_i a_{1ik} + z^2\sum_{i=1}^{3} g_i a_{2ik} + z^3\sum_{i=1}^{3} g_i a_{3ik}, \quad k = 1,2 \tag{1}$$

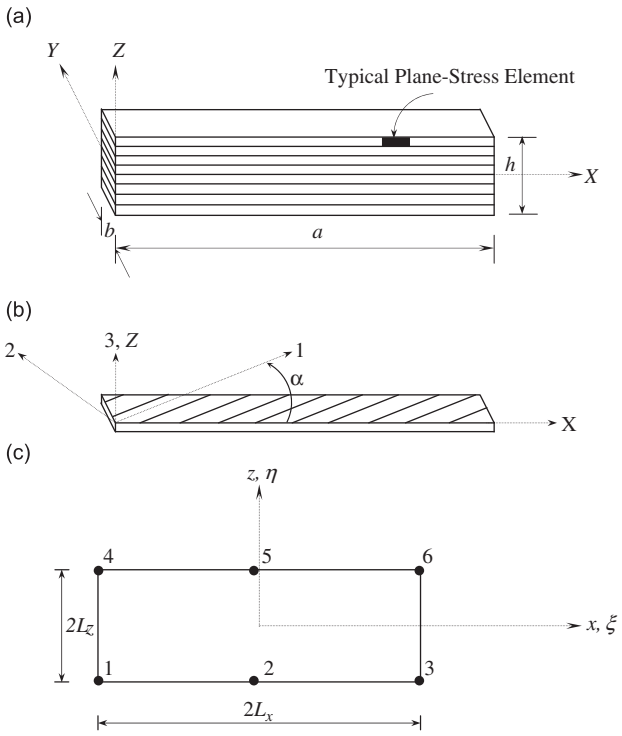

Fig. 1. (a) Geometry of composite laminated beam with positive set of reference axes. (b) Geometry of composite lamina (i.e. ply) with positive set of reference axes. (c) Geometry of six-node plane stress (2-D) element with positive set of reference axes.

where

$$g_1 = \frac{\xi}{2}(\xi - 1), \quad g_2 = 1 - \xi^2, \quad g_3 = \frac{\xi}{2}(1 + \xi), \quad \xi = x/L_x \tag{2}$$

and

$$u_1(x,z,t) = u(x,z,t); \quad u_2(x,z,t) = w(x,z,t) \tag{3}$$

Further, the generalized coordinates a_{mik} $(m = 0, 1, \ldots, 3)$ are functions of z and the element's coordinate axes x, z are parallel to the laminate coordinate system X, Z respectively.

Each lamina in the laminate has been considered to be in the state of plane stress in X–Z plane so that the constitutive relation for a typical ith lamina with reference to the element's coordinate system can be shown to be

$$\{\sigma\} = [D]\{\varepsilon\} \tag{4}$$

where

$$\{\sigma\} = [\sigma_x \ \ \sigma_z \ \ \tau_{xz}]^{\mathrm{T}}; \quad [D] = \begin{bmatrix} D_{11} & D_{13} & 0 \\ D_{13} & D_{33} & 0 \\ 0 & 0 & D_{55} \end{bmatrix} \quad \text{and} \quad \{\varepsilon\} = [\varepsilon_x \ \ \varepsilon_z \ \ \gamma_{xz}]^{\mathrm{T}} \tag{5}$$

The coefficients D_{mn} are the elastic constants in the element's axes x, y, z. The transverse stresses can be obtained from the constitutive Eq. (4) and strain displacement relations as

$$\sigma_z = D_{13}\varepsilon_x + D_{33}\varepsilon_z = D_{13}\frac{\partial u}{\partial x} + D_{33}\frac{\partial w}{\partial z} \quad \text{and} \quad \tau_{xz} = D_{55}\gamma_{xz} = D_{55}\left(\frac{\partial u}{\partial z} + \frac{\partial w}{\partial x}\right) \tag{6}$$

By using Eqs. (1) and (6), coefficients a_{mik} ($m = 0, 1, 2, 3$; $i = 1, 2, 3$ and $k = 1, 2$) can be determined and finally the displacement fields $u(x,z,t)$ and $w(x,z,t)$ can be expressed in terms of the nodal degrees-of-freedom as

$$\{u\} = [u \ \ w]^{\mathrm{T}} = [N]\{q\} \tag{7}$$

where

$$[N] = [\underline{N}_1 \ \ \underline{N}_2 \ \ \underline{N}_3 \ \ \underline{N}_4 \ \ \underline{N}_5 \ \ \underline{N}_6] \quad \text{and} \quad \{q\} = [\underset{\sim}{q}_1^{\mathrm{T}} \ \ \underset{\sim}{q}_2^{\mathrm{T}} \ \ \underset{\sim}{q}_3^{\mathrm{T}} \ \ \underset{\sim}{q}_4^{\mathrm{T}} \ \ \underset{\sim}{q}_5^{\mathrm{T}} \ \ \underset{\sim}{q}_6^{\mathrm{T}}]^{\mathrm{T}} \tag{8}$$

$$\{q_n\} = [u_n \ \ w_n \ \ (\tau_{xz})_n \ \ (\sigma_z)_n]^{\mathrm{T}} \quad \text{and} \quad [N_n] = \begin{bmatrix} g_i f_q & h_i f_p & g_i f_p \dfrac{1}{D_{55}} & 0 \\ h_i f_p \dfrac{D_{13}}{D_{33}} & g_i f_q & 0 & g_i f_p \dfrac{1}{D_{33}} \end{bmatrix} \tag{9}$$

Here, $i = 1, 2, 3$ for the nodes with $\xi = -1$, $\xi = 0$ and $\xi = 1$, respectively.

$p = 3$, $q = 1$ for the nodes with $\eta = -1$ and $p = 4$, $q = 2$ for the nodes with $\eta = 1$.

and

$$h_i = -\frac{\partial g_i}{\partial x}; \quad f_1 = \frac{1}{4}(2 - 3\eta + \eta^3); \quad f_2 = \frac{1}{4}(2 + 3\eta - \eta^3); \quad f_3 = \frac{L_z}{4}(1 - \eta - \eta^2 + \eta^3);$$
$$f_4 = \frac{L_z}{4}(-1 - \eta + \eta^2 + \eta^3); \quad \eta = z/L_z \tag{10}$$

In the absence of external and damping forces (i.e. undamped natural vibration), the total energy of an element within a lamina can be given by

$$L^e = T^e - U^e \tag{11}$$

Here, U_e and T_e represent the internal strain and kinetic energies, respectively. Functional in Eq. (11) can be expressed in the matrix form for linear elastic system as

$$L^e = \frac{1}{2}\left[\int \rho\{\dot{u}\}^{\mathrm{T}}\{\dot{u}\}\,\mathrm{d}v - \int \{\varepsilon\}^{\mathrm{T}}\{\sigma\}\,\mathrm{d}v\right] \tag{12}$$

where ρ is the mass density of the material, and $\{\dot{u}\} = \mathrm{d}\{u\}/\mathrm{d}t$

The strain vector $\{\varepsilon\}$ and the stress vector $\{\sigma\}$ can be expressed as

$$\{\varepsilon\} = [B]\{q\} \quad \text{and} \quad \{\sigma\} = [D][B]\{q\} \tag{13}$$

where

$$[B] = [\underline{B}_1 \ \ \underline{B}_2 \ \ \underline{B}_3 \ \ \underline{B}_4 \ \ \underline{B}_5 \ \ \underline{B}_6] \tag{14}$$

and

$$[B_n]=\begin{bmatrix}\dfrac{\partial}{\partial x} & 0\\ 0 & \dfrac{\partial}{\partial z}\\ \dfrac{\partial}{\partial z} & \dfrac{\partial}{\partial x}\end{bmatrix}[N_n]=\begin{bmatrix}-h_i f_q & h_i' f_p & -h_i f_p\dfrac{1}{D_{55}} & 0\\ h_i \bar{f}_p\dfrac{D_{13}}{D_{33}} & g_i \bar{f}_q & 0 & g_i \bar{f}_p\\ g_i \bar{f}_q + h_i' f_p\dfrac{D_{13}}{D_{33}} & h_i \bar{f}_p - h_i f_q & g_i \bar{f}_p\dfrac{1}{D_{55}} & -h_i \bar{f}_p\dfrac{1}{D_{33}}\end{bmatrix} \tag{15}$$

Furthermore

$$h_i'=\frac{\partial h_i}{\partial x};\quad \bar{f}_j=\frac{\partial f_j}{\partial z};\quad j=p \text{ or } q \tag{16}$$

By summing up the total energies over all the elements and applying Hamilton's principle [13]

$$\delta\int_{t_1}^{t_2} L\,\mathrm{d}t=0 \tag{17}$$

where $L=\sum_e L_e$ and δ implies first variation. The global equation of motion, in the absence of external forces, can be obtained as

$$[M]\{\ddot{Q}\}+[K]\{Q\}=0 \tag{18}$$

Here, global inertia matrix $[M]$, global property matrix $[K]$, and global nodal degrees-of-freedom vector $\{Q\}$ are defined as

$$[M]=\sum_e [M]_e;\quad [K]=\sum_e [K]_e;\quad \{Q\}=\sum_e \{q\}; \tag{19}$$

where

$$[M_e]=\rho\int [N]^{\mathrm{T}}[N]\,\mathrm{d}v;\quad [K_e]=\int [B]^{\mathrm{T}}[D][B]\,\mathrm{d}v \quad\text{and}\quad \{\ddot{Q}\}=\frac{\mathrm{d}^2\{Q\}}{\mathrm{d}t^2} \tag{20}$$

For harmonic vibrations, the general solution of equation of motion (18) can be considered of the form $\{Q\}=\{\hat{Q}\}\mathrm{e}^{\mathrm{i}\omega t}$, where $\{\hat{Q}\}$ is the modal vector and ω is the natural frequency. On substitution Eq. (18) results in the following generalized eigenvalue problem

$$([K]-\omega^2[M])\{\hat{Q}\}=0 \tag{21}$$

Solution of Eq. (21) yields the natural frequency ω and the corresponding eigenvector $\{\hat{Q}\}$ after the imposition of boundary conditions.

2.2. Models for analysis of composite laminated beams with delamination

The two models namely the *unconstrained-interface model* and the *contact-interface model* has been developed for the free vibrations of delaminated beams. Fig. 2(a) shows the cross section of a laminated beam with delamination at an arbitrary location. The finite element meshing of the beam is also shown in the figure. Because of high stress concentration near delamination, finer mesh is proposed in these regions. As shown in Fig. 2(b), the elements have been separated at the delaminated region by allocating different node numbers to the nodes on the lower and the upper delaminated interfaces. However in the regions with no delamination the usual pattern of node numbering has been followed. Following is the description for the two models developed for the analysis of delaminated beams.

Unconstrained-interface model: This model is based on the assumption that there is no contact between the upper and the lower interfaces in the delaminated region. It implies that the upper and the lower layers in this region are free to undergo the transverse displacements as per their condition of equilibrium without considerations of constraints imposed by the adjacent layers. This may lead to overlapping of the upper and the lower layers in the delaminated region, thereby violating the compatibility of deformation. Based on the assumed conditions, all the displacement degrees-of-freedom u and w have been kept unrestrained at the nodes on the upper and the lower delaminated interfaces. The no-contact condition between the upper and the lower interface at the delaminated region is imposed by explicitly setting the transverse stress degrees-of-freedom τ_{xz} and σ_z to zero.

Contact-interface model: The upper and the lower delaminated interfaces have been assumed to be in contact along the delaminated region and the coupling effect is accounted for both the upper as well as the lower interfaces at the delaminated region in this model. The tendency of one of the delaminated layer to overlap the other layer will be resisted by the development of a contact pressure distribution between the adjacent layers through this model. Thus the model will be able to ensure compatibility of deformation. The coupling between the transverse displacement 'w' and the transverse normal stress 'σ_z' throughout the delaminated region have been ensured by the pre and the post multiplication of the transpose of transformation matrix i.e. $[T_d]^{\mathrm{T}}$ and the transformation matrix $[T_d]$, respectively, to the global property matrix $[K]$ and the global inertia matrix $[M]$. However, the transverse shear stress degrees-of-freedom τ_{xz} has been explicitly set to

zero, assuming the upper and the lower delaminated interfaces to be frictionless. The in-plane displacement 'u' has been kept unrestrained. The mathematical operation involved in the transformation of the global property matrix [K] and the global inertia matrix [M] is shown below.

A typical form of the transformation matrix [T_d] has been presented here which is for a typical set of upper-lower nodes (shown with the symbol ◉ on the upper and the lower delaminated interfaces in Fig. 2(b)). The degrees-of-freedom at the typical node on the upper delaminated interface are u_u, w_u, τ_{xzu} and σ_{zu}. On the other hand u_l, w_l, τ_{xzl} and σ_{zl} are the degrees-of-freedom at the typical node on the lower delaminated interface. The typical transformation matrix [T_d] can be obtained as

$$[T_d] =$$

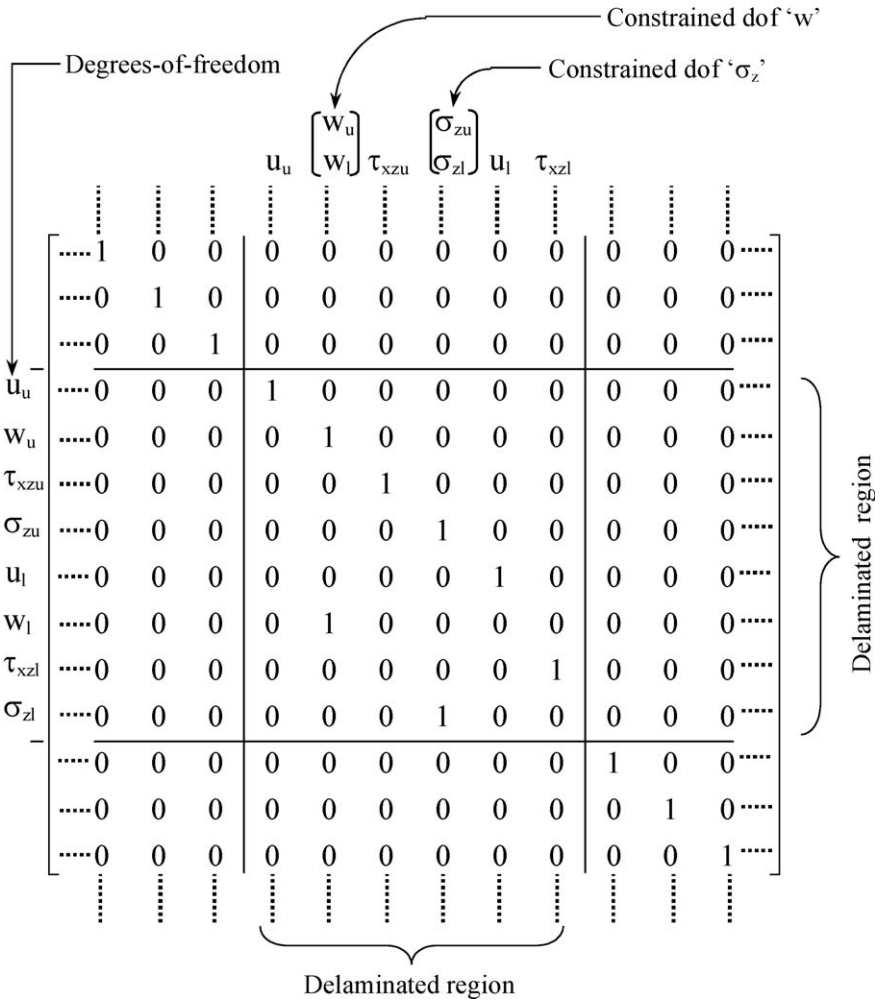

(22)

The modified global property matrix [K_m] and the modified global inertia matrix [M_m] are given by

$$[K_m] = [T_d]^{\mathrm{T}}[K][T_d];$$

$$[M_m] = [T_d]^{\mathrm{T}}[M][T_d]; \tag{23}$$

where [K] and [M] are the global property and inertia matrices, respectively.

3. Numerical investigations

Numerical investigations have been undertaken for the free vibrations of layered isotropic as well as cross-ply laminated beams having delamination at specified locations. The analysis has been conducted using two models namely *unconstrained-interface model* and *contact-interface model*. The boundary conditions and the material properties are tabulated in Tables 1 and 2, respectively.

Illustrative examples are discussed in the following paragraphs,

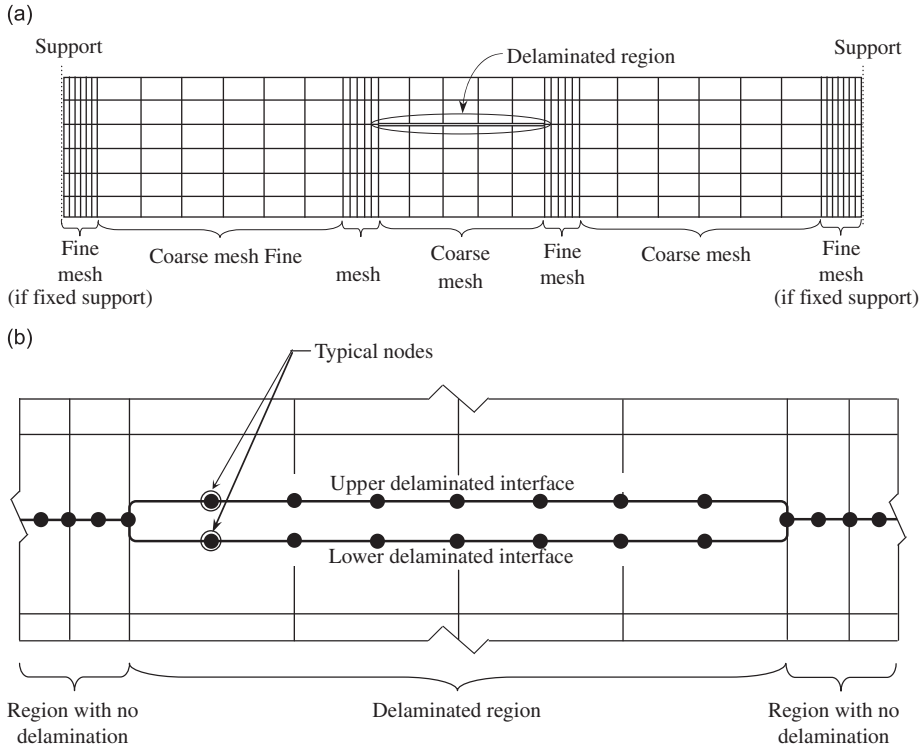

Fig. 2. (a) Cross-section of a composite laminate showing delaminated region and typical finite element meshing. (b) Delaminated region (exaggerated) showing finite element nodes.

Table 1
Boundary conditions.

Description	Location	Degree-of-freedom			
		u	w	τ_{xz}	σ_z
(a) Beam with delamination under clamped supports at both the ends	$X=0$ and $X=a$	0	0	–	–
	$Z=\pm h/2$	–		0	0
	At delaminated interface of upper and lower layer:				
	(i) Unconstrained-interface model	–	–	0	0
	(ii) Contact-interface model	–	$w_u=w_l$	0	$\sigma_{zu}=\sigma_{zl}$
(b) Beam with delamination under clamped-free supports condition	$X=0$	0	0	–	0
	$X=a$	–	–	0	–
	$Z=\pm h/2$	–	–	0	0
	At delaminated interface of upper and lower layer:				
	(i) Unconstrained-interface model	–	–	0	0
	(ii) Contact-interface model	–	$w_u=w_l$	0	$\sigma_{zu}=\sigma_{zl}$

Note: (i) '–' indicates no boundary condition imposed on that degree-of-freedom at that location.
(ii) w_u, w_l are the transverse displacement and σ_u, σ_l are the transverse normal stress degree-of-freedom at the upper and the lower delaminated interface, respectively.

Example 1. An isotropic ($v=0.3$) thin beam shown in Fig. 3 has been considered for free vibration analysis. The beam is provided with the clamped–clamped supports for which the imposed boundary conditions are tabulated in Table 1(a). The free vibration analysis using the *unconstrained-interface model* has been conducted for various mid-plane delaminations (i.e. $h_t/h=0.5$) located at the centre of the beam (i.e. $a_l/a=0.5$). The non-dimensional natural frequencies $\bar{\omega}$ ($\bar{\omega}=\omega a^2\sqrt{\rho h/EI}$) for the first three modes are presented in Table 3 along with the results produced by Wang et al. [2] and those by Lee [8]. The results from the present analysis have been found in good agreement with the available results.

Table 2
Material properties.

Example	Source	Properties
3	Shen and Grady [5]	$E_1 = 134.49\,\text{GPa}$; $E_3 = 10.34\,\text{GPa}$; $G_{13} = 5.00\,\text{GPa}$; $v = 0.3$; $\rho = 1477.60\text{E}{-12}\,\text{N s}^2/\text{mm}^4$

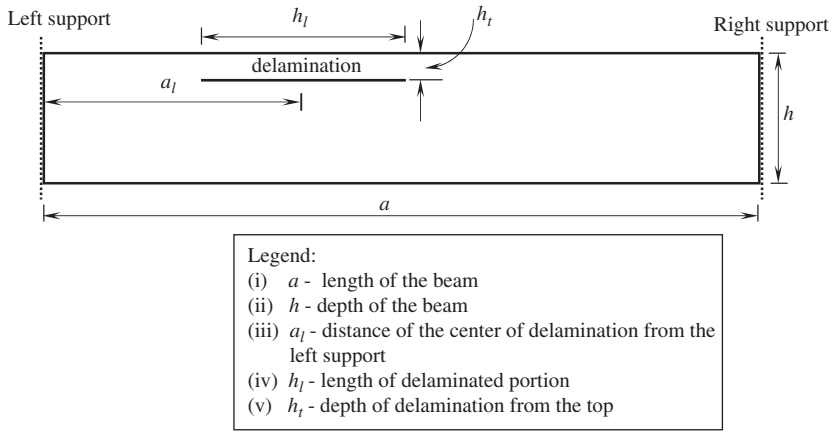

Fig. 3. Geometry of the delaminated beam.

Table 3
Natural frequencies of a clamped beam with a mid-plane delamination ($a_l = a/2$) for various h_l/a.

h_l/a	Present analysis [unconstrained-interface model]			Wang et al. [2]			Lee [8]		
	$\bar{\omega}_1$	$\bar{\omega}_2$	$\bar{\omega}_3$	$\bar{\omega}_1$	$\bar{\omega}_2$	$\bar{\omega}_3$	$\bar{\omega}_1$	$\bar{\omega}_2$	$\bar{\omega}_3$
0.0	22.39	61.81	121.36	22.39	61.67	120.91	22.36	61.61	120.68
0.1	22.37	60.93	120.87	22.37	60.76	120.81	22.36	60.74	120.62
0.2	22.36	56.10	119.19	22.35	55.97	118.76	22.35	55.95	118.69
0.3	22.23	48.97	109.19	22.23	49.00	109.04	22.23	48.97	109.03
0.4	21.67	44.56	93.51	21.83	43.87	93.57	21.82	43.86	93.51
0.5	20.88	41.51	82.31	20.88	41.45	82.29	20.88	41.50	82.23
0.6	19.31	41.10	77.91	19.29	40.93	77.64	19.28	41.01	77.64
0.7	17.22	40.84	77.25	17.23	40.72	77.05	17.22	40.80	77.12
0.8	15.06	39.18	75.83	15.05	39.01	75.33	15.05	39.04	75.39
0.9	12.99	35.41	69.30	13.00	35.38	69.17	12.99	35.38	69.16

Example 2. An isotropic ($v = 0.3$) thin beam with off-midplane delamination ($h_t/h = 0.33$) shown in Fig. 3 has been considered for free vibrations. The beam is supported under the clamped-free boundary conditions as tabulated in Table 1(b). The free vibrations have been investigated using the *unconstrained-interface model* and the *contact-interface model*; and the frequencies for the first two modes are reported in Table 4. It can be observed that the frequencies computed by the *contact-interface model* for the first as well as second mode closely matches with the experimental results obtained by Mujumdar and Suryanarayan [3]. For the first mode of vibration, the *unconstrained-interface model* has also been found to yield frequencies, matching with the experimental results. However, for the second mode, the *unconstrained-interface model* yields low frequencies in comparison to the experimental results. The reason for this discrepancy may be attributed to the fact that the influence of individual delaminated layer becomes more pronounced in case of the *unconstrained-interface model* for higher modes of vibrations. Thus the beam tends to be relatively more flexible. However, in case of the *contact-interface model*, because the upper and the lower layers are constrained to act together by imposing the condition of constrained transverse displacement 'w' and transverse normal stress 'σ_z', the beam maintains its structural property (flexibility) even at higher modes of vibrations.

Example 3. An eight-layer symmetric cross-ply laminated $(0^\circ/90^\circ)_{2s}$ beam, under the clamped-free supports is considered for analysis. Boundary conditions are tabulated in Table 1(b), whereas the material properties are given in Table 2. The beam showing various interfaces and dimensions is shown in Fig. 4. Free vibration analysis has been conducted by employing the *unconstrained-interface* and the *contact-interface models* on the beam with single delamination of varying

Table 4
Comparison of the experimental and the theoretical frequencies of cantilever beam with an off-midplane delamination ($h_t/h = 0.33$).

Specimen span (mm)	Dimension		First mode					Second mode				
	a_l (mm)	h_l (mm)	Experiment (Mujumdar and Suryanarayan [3])	Mujumdar and Suryanarayan [3]		Present analysis		Experiment (Mujumdar and Suryanarayan [3])	Mujumdar and Suryanarayan [3]		Present analysis	
				Constrained mode (Hz)	Free mode (Hz)	Contact-interface model (Hz)	Unconstrained-interface model (Hz)		Constrained mode (Hz)	Free mode (Hz)	Contact-interface model (Hz)	Unconstrained-interface model (Hz)
240.0	153.5	96.0	31.6	32.37	32.26	31.14	31.11	172.1	176.46	159.86	171.00	156.24
250.0	104.0	148.0	31.7	31.99	31.98	31.49	31.51	190.5	200.67	198.74	197.88	197.23
175.0	133.0	88.5	56.9	58.06	57.97	56.45	56.35	339.3	346.35	248.96	337.49	244.42
200.0	122.0	106.0	46.6	47.21	47.18	46.37	46.34	291.0	297.06	260.88	292.43	258.95
155.0	122.0	61.0	69.1	69.95	69.93	69.93	68.82	363.7	361.63	281.76	361.76	249.20
225.0	134.0	138.0	40.1	39.57	39.54	39.73	39.51	237.9	243.66	223.13	236.91	222.20
200.0	134.0	113.0	49.6	48.46	48.40	48.61	48.47	297.3	302.51	241.96	299.46	238.28
175.0	134.0	88.0	60.6	59.57	59.48	59.56	59.50	358.6	354.17	247.87	356.74	247.65

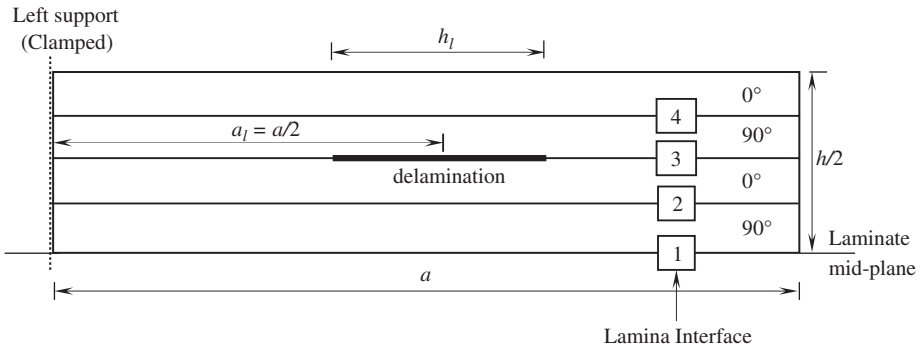

Fig. 4. Geometry of the eight layer symmetric composite laminated beam $[(0^\circ/90^\circ)_{2s}]$ showing various interfaces for delamination.

length and at different interfaces. The frequencies for the first two modes of vibration are tabulated in Table 5–8. The fundamental frequencies obtained through the experiment and the theoretical models by Shen and Grady [5] are also been presented in the table for proper comparison. It has been observed that the fundamental frequencies obtained by both the present models closely matches with the experimental results as well as with the *model-A* of Shen and Grady [5] for all the cases. However, the frequencies obtained by the present two models differ significantly with each other for the second mode of vibration. The *unconstrained-interface model* has been found to yield low frequencies for the second mode, as compared to those obtained by the *contact-interface model*, particularly, for the cases with off-midplane delamination (Tables 6–8). To ascertain the reason for this discrepancy, mode shapes showing the variation of the normalized displacements $\bar{W}$ and $\bar{U}$ as well as the stresses $\bar{\sigma}_Z$ and $\bar{\tau}_{XZ}$ along the length at the delaminated interface are drawn. Figs. 5(a–d) and 6(a–d) show these variations for the first and second modes of vibrations for the beam with delamination length $a_l = 76.2$ mm, at the interface 3, respectively. It is interesting to note that both the models resulted into similar mode shapes for the first mode of vibration. For this mode, similar to the *contact-interface model*, the *unconstrained-interface model* has also been found to maintain the compatibility of transverse displacement $\bar{W}$ at the delaminated interface (Fig. 5(a)). However, under the second mode of vibration, the *unconstrained-interface model* fails to maintain the deformation compatibility. It has been found to yield overlapping of transverse displacements $\bar{W}$ of the upper and the lower layers at the delaminated region (Fig. 6(a)). Similarly the variations of the in-plane displacement $\bar{U}$ and the stresses $\bar{\sigma}_Z$ and $\bar{\tau}_{XZ}$ along the length of the beam, as depicted by the *unconstrained-interface model* in Fig. 6(b–d) show unrealistic variation in the delaminated region, whereas the *contact-interface model* has been found to present a realistic mode shapes under both the modes of vibrations.

From the observations of Examples 2 and 3, it can be concluded that the *unconstrained-interface model* is not suitable for the analyses of the delaminated beams, particularly with off-midplane delamination. The *contact-interface model* has been found to represent reasonably correct behaviour of the delaminated beams.

Table 5
Natural frequencies of eight-layer cross-ply laminated beam with delamination along interface 1.

Specimen dimension ($a = 127.0$ mm, $b = 12.70$ mm, $h = 1.016$ mm)		Fundamental frequency (in Hz)							Frequency in mode 2 (in Hz)	
		Experimental (Shen and Grady [5])			Analytical model (Shen and Grady [5])		Present analysis		Present analysis	
a_l (mm)	h_l (mm)	Specimen 1	Specimen 2	Specimen 3	Model A[a]	Model B[b]	Unconstrained-interface model	Contact-interface model	Unconstrained-interface model	Contact-interface model
63.50	0.00	79.875	79.875	79.750	82.042	82.042	81.873	81.873	519.238	519.238
63.50	25.4	78.376	79.126	77.001	80.133	67.363	81.229	81.229	515.166	515.166
63.50	50.8	74.375	75.000	76.751	75.285	56.479	76.601	76.601	492.376	492.376
63.50	76.2	68.250	66.250	66.375	66.936	47.898	67.471	67.471	420.406	420.406
63.50	101.6	57.623	57.502	57.501	57.239	40.586	56.891	56.891	329.402	329.402

[a] Crack interfaces is assumed to be in contact along the delaminated region throughout the vibration and the coupling effect is accounted for in both the upper and lower plies in the delaminated region.
[b] The contact between the delamination surfaces is neglected.

Table 6
Natural frequencies of eight-layer cross-ply laminated beam with delamination along interface 2.

Specimen dimension ($a = 127.0$ mm, $b = 12.70$ mm, $h = 1.016$ mm)		Fundamental frequency (in Hz)							Frequency in mode 2 (in Hz)	
		Experimental (Shen and Grady [5])			Analytical model (Shen and Grady [5])		Present analysis		Present analysis	
a_l (mm)	h_l (mm)	Specimen 1	Specimen 2	Specimen 3	Model A[a]	Model B[b]	Unconstrained-interface model	Contact-interface model	Unconstrained-interface model	Contact-interface model
63.50	25.4	78.375	78.375	76.626	81.385	68.776	81.285	81.285	515.265	515.270
63.50	50.8	75.126	75.250	75.001	78.103	59.438	76.978	76.980	493.949	494.048
63.50	76.2	64.001	70.001	69.876	71.159	51.180	68.330	68.335	425.078	425.736
63.50	101.6	45.752	49.751	49.502	62.121	43.860	57.971	57.977	329.115	334.136

[a] Crack interfaces is assumed to be in contact along the delaminated region throughout the vibration and the coupling effect is accounted for in both the upper and lower plies in the delaminated region.
[b] The contact between the delamination surfaces is neglected.

Table 7
Natural frequencies of eight-layer cross-ply laminated beam with delamination along interface 3.

Specimen dimension ($a = 127.0$ mm, $b = 12.70$ mm, $h = 1.016$ mm)		Fundamental frequency (in Hz)							Frequency in mode 2 (in Hz)	
		Experimental (Shen and Grady [5])			Analytical model (Shen and Grady [5])		Present analysis		Present analysis	
a_l (mm)	h_l (mm)	Specimen 1	Specimen 2	Specimen 3	Model A[a]	Model B[b]	Unconstrained-interface model	Contact-interface model	Unconstrained-interface model	Contact-interface model
63.50	25.4	79.625	80.125	80.625	81.461	75.137	81.729	81.733	513.233	514.131
63.50	50.8	79.500	81.875	77.875	79.932	70.416	80.462	80.508	440.304	508.608
63.50	76.2	75.625	77.125	78.125	76.712	65.058	77.359	77.544	226.024	486.747
63.50	101.6	73.376	73.627	70.376	71.663	59.131	71.604	72.955	128.555	436.956

[a] Crack interfaces is assumed to be in contact along the delaminated region throughout the vibration and the coupling effect is accounted for in both the upper and lower plies in the delaminated region.
[b] The contact between the delamination surfaces is neglected.

4. Conclusions

The free vibrations of delaminated composite beams have been presented in this paper. The 2-D (plane-stress) mixed finite element model developed by the authors [1] has been employed with the two conceptual models for delaminated portion of the beam, namely the *unconstrained-interface* and the *contact-interface models*. Because the mixed finite element

Table 8
Natural frequencies of eight-layer cross-ply laminated beam with delamination along interface 4.

Specimen dimension ($a = 127.0$ mm, $b = 12.70$ mm, $h = 1.016$ mm)		Fundamental frequency (in Hz)							Frequency in mode 2 (in Hz)	
		Experimental (Shen and Grady [5])			Analytical model (Shen and Grady [5])		Present analysis		Present analysis	
a_l (mm)	h_l (mm)	Specimen 1	Specimen 2	Specimen 3	Model A[a]	Model B[b]	Unconstrained - interface model	Contact-interface model	Unconstrained - interface model	Contact-interface model
63.50	25.4	75.375	75.250	77.250	81.598	75.834	81.753	81.754	513.729	514.166
63.50	50.8	69.376	68.001	69.375	80.383	71.881	80.727	80.743	476.638	510.323
63.50	76.2	65.375	59.625	–	77.698	67.181	77.887	78.024	227.614	487.668
63.50	101.6	52.750	57.876	56.251	73.147	61.704	73.090	73.783	126.076	441.835

[a] Crack interfaces is assumed to be in contact along the delaminated region throughout the vibration and the coupling effect is accounted for in both the upper and lower plies in the delaminated region.
[b] The contact between the delamination surfaces is neglected.

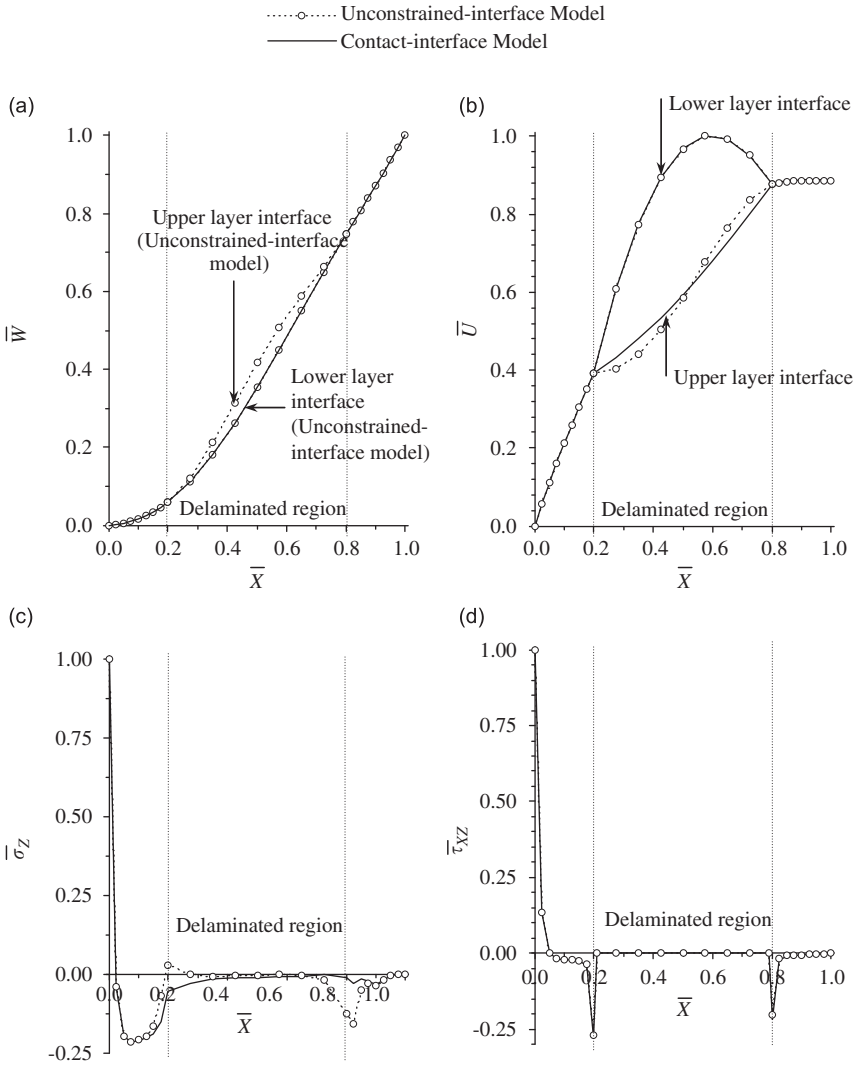

Fig. 5. Variation of the normalized (a) $\bar{W}$, (b) $\bar{U}$, (c) $\bar{\sigma}_Z$, and (d) $\bar{\tau}_{XZ}$ along the length of the beam (i.e. X-axis), at the delaminated interface 3, under the fundamental mode (i.e. mode 1) of vibration.

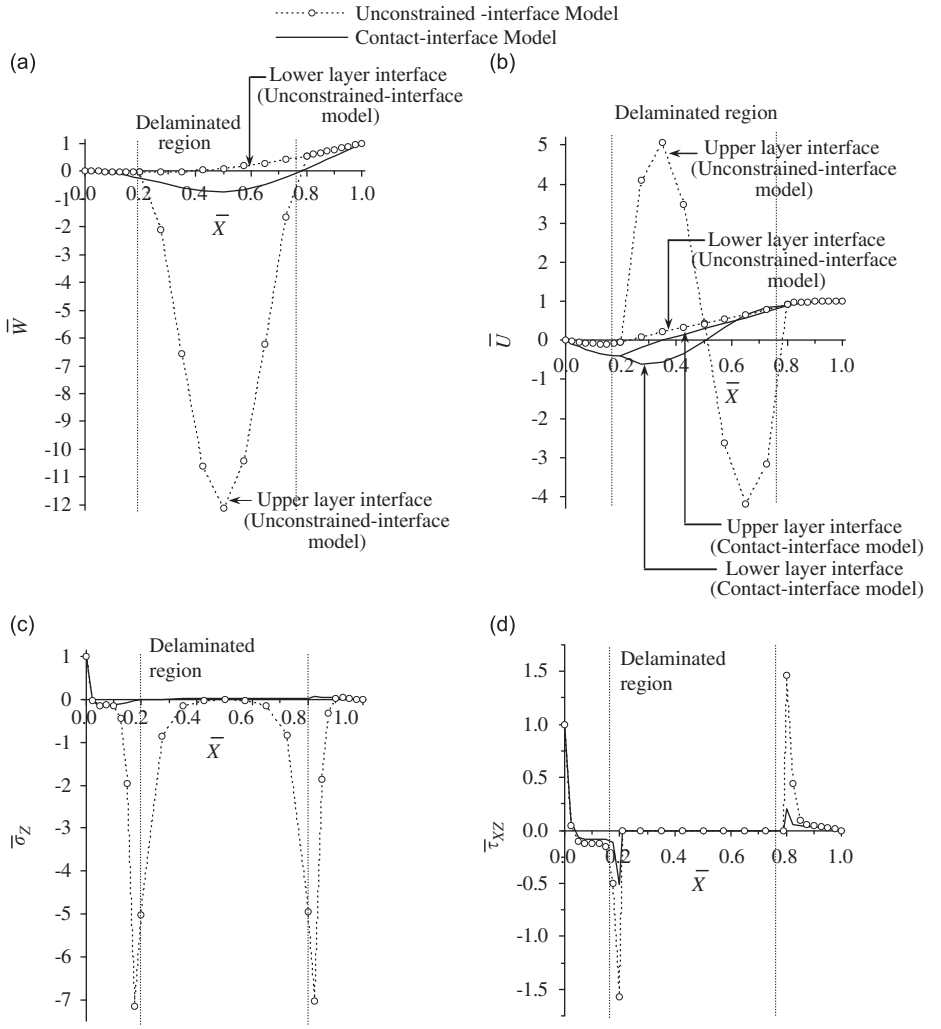

Fig. 6. Variation of the normalized (a) $\bar{W}$, (b) $\bar{U}$, (c) $\bar{\sigma}_Z$, and (d) $\bar{\tau}_{XZ}$ along the length of the beam (i.e. *X*-axis), at the delaminated interface 3, under the second mode (i.e. mode 2) of vibration.

model contains the transverse stress components as the nodal variables along with the displacement variables, it aptly maps the elastic behaviour of laminated composite beams with delamination. Based on the numerical investigations following conclusions may be drawn.

- Excellent correlation with the experimental results has been obtained through the *contact-interface model*. This validates the model. The variation of the transverse stresses along the length of the beam at the delaminated interface show shooting of these stresses at the delamination fronts, which increases with the higher mode of vibrations.
- The *unconstrained-interface model* in which the contact between the upper and the lower layers at the delaminated interface has been neglected during the vibration, does not present a realistic behaviour of the beam, particularly at the higher mode of vibrations.
- The present analysis could easily be extended to the laminated beams with multiple delaminations. Further, the present mixed FE model along with the *contact-interface model* could be utilized for an inverse analysis to identify the delamination properties from dynamical measurements.

References

[1] G.S. Ramtekkar, Y.M. Desai, A.H. Shah, Natural vibrations of laminated composite beams by using mixed finite element modeling, *Journal of Sound and Vibration* 257 (4) (2002) 635–641.
[2] J.T.S. Wang, Y.Y. Liu, J.A. Gibby, Vibrations of split beams, *Journal of Sound and Vibration* 84 (4) (1982) 491–502.
[3] P.M. Mujumdar, S. Suryanarayan, Flexural vibrations of beams with delaminations, *Journal of Sound and Vibration* 125 (3) (1988) 441–461.

[4] J.J. Tracy, G.C. Pardoen, Effect of delamination on the natural frequencies of composite laminates, *Journal of Composite Materials* 23 (1989) 1200–1215.
[5] M.H.H. Shen, J.E. Grady, Free vibrations of delaminated beams, *AIAA Journal* 30 (5) (1992) 1361–1370.
[6] J.S. Hu, C. Hwu, Free vibration of delaminated composite sandwich beams, *AIAA Journal* 33 (10) (1995) 1911–1918.
[7] M. Krawczuk, W. Ostachowicz, A. Zak, Analysis of natural frequencies of delaminated composite beams based on finite element method, *Journal of Engineering Mechanics* 4 (3) (1996) 243–255.
[8] J. Lee, Free vibration analysis of delaminated composite beams, *Computers and Structures* 74 (2000) 121–129.
[9] Y. Zou, L. Tong, G.P. Steven, Vibration-based model-dependent damage (delamination) identification and health monitoring for composite structures—A review, *Journal of Sound and Vibration* 230 (2) (2000) 357–378.
[10] A. Karmakar, H. Roy, K. Kishimoto, Free vibration analysis of delaminated composite pretwisted shells, *Aircraft Engineering and Aerospace Technology* 77 (6) (2005) 486–490.
[11] C.N. Della, D. Shu, Vibration of delaminated composite laminates: a review, *Applied Mechanics Reviews* 60 (1) (2007) 1–20.
[12] C.N. Della, D. Shu, Free vibration analysis of multiple delaminated beams under axial compressive load, *Journal of Reinforced Plastics and Composites* (2008) doi:10.1177/0731684408089503.
[13] K.J. Bathe, *Finite Element Procedures*, Prentice-Hall of India, New Delhi, 1997.